

College of Saint Benedict and Saint John's University

DigitalCommons@CSB/SJU

Honors Theses, 1963-2015

Honors Program

5-1-2015

Identification, Synthesis and Biological Activity of Galloyl Inhibitors of Human Low Molecular Weight Protein Tyrosine Phosphatase

Samuel T. Klinker

College of Saint Benedict/Saint John's University

Follow this and additional works at: https://digitalcommons.csbsju.edu/honors_theses

 Part of the [Chemistry Commons](#)

Recommended Citation

Klinker, Samuel T., "Identification, Synthesis and Biological Activity of Galloyl Inhibitors of Human Low Molecular Weight Protein Tyrosine Phosphatase" (2015). *Honors Theses, 1963-2015*. 87.

https://digitalcommons.csbsju.edu/honors_theses/87

This Thesis is brought to you for free and open access by DigitalCommons@CSB/SJU. It has been accepted for inclusion in Honors Theses, 1963-2015 by an authorized administrator of DigitalCommons@CSB/SJU. For more information, please contact digitalcommons@csbsju.edu.

Identification, Synthesis and Biological Activity of Galloyl Inhibitors of Human Low Molecular
Weight Protein Tyrosine Phosphatase

An Honors Thesis

In Partial Fulfillment
of the Requirements for Distinction
in the Department of Chemistry

By: Samuel T. Klinker

May 1, 2015

Identification, Synthesis and Biological Activity of Galloyl Inhibitors of Human Low Molecular Weight Protein Tyrosine Phosphatase

Samuel T. Klinker, Edward J. McIntee, Henry V. Jakubowski

Abstract

Low Molecular Weight Protein Tyrosine Phosphatase (LMW-PTP) isoform 2 (IF2) has been found to be over expressed in many forms of aggressive cancer and has become a target for inhibition. Competitive inhibition of LMW-PTP IF2 by known inhibitor pyridoxal-5'-phosphate (PLP) shows a strong inhibition constant ($K_i = 7.6 \mu\text{M}$ at pH 5.0); however, PLP is a cofactor for many other enzymes. *In silico* screening and *in vitro* testing identified NSC107022 ($K_i = 10.8 \pm 1.0$) from the National Cancer Institute's Diversity Set II as a lead compound for optimization as a LMW-PTP IF2 inhibitor. Utilizing NSC107022's galloyl group, compound libraries of aromatic alcohols and amines were connected (ester and amide linkages, respectively) and screened *in silico*. Twelve compounds, eight esters and four amides yielding top docking scores (most negative) were selected for synthesis and *in vitro* screening.

Introduction

Post-translation phosphorylation of protein Ser, Thr and Tyr residues is an important reversible modification that plays a central role in eukaryotic cellular activities such as cell growth, proliferation, differentiation, migration and gene expression.¹ The phosphorylation and dephosphorylation of tyrosine residues is under dynamic control of protein tyrosine kinases (PTKs) and protein tyrosine phosphatases (PTPs), respectively. The human genome codes for 107 known PTPs which can be classified into four subgroups: classical pTyr specific, dual specificity, Cdc25 and low molecular weight protein tyrosine phosphatases (LMW-PTP).^{2,3} All PTPs share a common active site phosphate binding P-loop (CX₅R(S/T)) and catalytic mechanism involving a crucial cysteine residue but differ greatly in tertiary structure, sequence and specificity.² The LMW-PTP subgroup has recently emerged as a novel drug target due to their involvement in metabolic and tumor regulation.¹

LMW-PTPs are 18 kDa enzymes with no particular tissue specificity belonging to class II cysteine based PTPs.⁴ Human LMW-PTP is active downstream in growth factor signaling pathways and is linked to cellular transformation and tumor onset.^{2,3,5,6} LMW-PTP mRNA and protein levels are shown to be highly increased in human breast, kidney, colon and bladder tumor

samples.⁷ Moreover, overexpression of LMW-PTP causes neoplastic cellular transformation and cancer progression.⁵ Likewise, increased levels of LMW-PTP is characteristic of more aggressive cancer.^{8,9}

LMW-PTP gains its oncogenic potential through expression of the ephrin A2 (EphA2) receptor tyrosine kinase.⁶ The overexpression of EphA2 is linked to many types of aggressive and metastatic cancers. Dephosphorylated EphA2 promotes cellular migration and tumor onset. In cancer cells, overexpression of LMW-PTP is a crucial EphA2 regulator and in turn leads to high levels of dephosphorylated EphA2 which triggers neoplastic transformation of non-transformed cells.^{1,5} Likewise, the action of LMW-PTP on EphA2 reduces its ability to dephosphorylate p190Rho-GAP which is critical for cell-matrix adhesion.² The Rho family of GTPases are important regulators of cell migration and this weakened adhesion leads to greater cell motility and migration.¹⁰

The LMW-PTP family is found as four different isozymes: two active forms, isoform 1 (also known as IFA, HCPTA or *fast*) and isoform 2 (also known as IFB, HCPTB or *slow*), and two catalytically inactive forms, IFC and SV3 (splicing variant 3). The two active isoforms are derived from alternative splicing of the same primary RNA transcript and differ only in sequence of residues 40-73.³ This section flanks the catalytic active site and determines ligand specificity and modulation for the isoforms. Thus, different cellular functions have been suggested for isoform 1 and 2.^{11,12} Recently, data has shown the isoforms have opposite roles in tumorigenesis, where isoform 1 is anti-oncogenic and isoform 2 is oncogenic.¹³

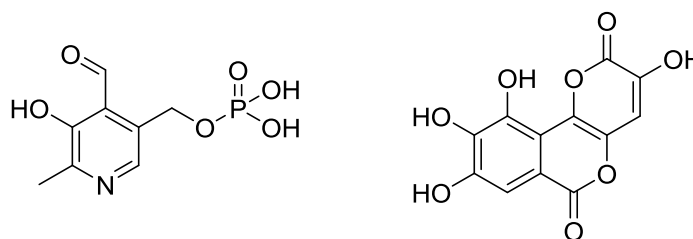


Fig. 1. Structures of PLP and NSC107022, respectively.

Few inhibitors for human LMW-PTP have been discovered due to its relatively recent discovery as a novel drug target. Pyridoxal 5'-phosphate (PLP, Fig 1) is a known inhibitor of LMW-PTP which displays tight binding ($K_i=7.6 \mu\text{M}$, pH 5).¹⁴ Unfortunately, PLP is a necessary cofactor for a plethora of enzymes and lacks the specificity required to inhibit LMW-PTP. Virtual screening of compound libraries has emerged as a useful technique to help increase the

speed of identification of potential inhibitors for LMW-PTP.^{4,9} Seiler et al. utilized *in silico* docking methods to analyze the National Cancer Institute's (NCI) Diversity Sets II and III and screened potential compounds *in vitro*. NSC107022 (Fig 1) of NCI Diversity Set II showed similar binding to that of PLP ($10.8 \pm 1.0 \mu\text{M}$, pH 5.5)⁴ and was chosen for optimization. Utilizing the galloyl core of NSC107022 libraries of aryl alcohols and aromatic primary amines were coupled and docked *in silico*. Top molecules were subject to further docking then selected for synthesis and *in vitro* evaluation.

Results and Discussion

Compound libraries of aryl alcohols (approx. 3,000 molecules) and primary aromatic amines (approx. 3,500 molecules) obtained from Sigma-Aldrich were coupled to a galloyl base and docked into LMW-PTP IF2 *in silico*. The original screening process revealed ester linkages with a β -amino acid motif displayed the best docking scores, better than that of PLP shown in figure 2. After further *in silico* docking seven β -amino acids were selected for synthesis. 3-Amino-3-(3-methoxy-4-((3,4,5-trihydroxybenzoyl)oxy)phenyl)propanoic acid showed the best docking score (-10.401). Key interactions with LMW-PTP IF2 include hydrogen bonds of the galloyl hydroxyl groups with Trp49 along with π - π bonding with the same residue. The amino group of the molecule hydrogen bonded with Asp129 while the carboxyl group hydrogen bonded with Arg18 through the carbonyl and Cys17 and Ile16 through the deprotonated oxygen (Fig. 7). These interactions are different from that of NSC107022 (Fig. 3) with only Asp129 and Arg18 being in common. This points to a different orientation in the active site; however, the immense amount of hydrogen bonding relates to the better docking score when compared to NSC107022 as seen in Table 1. The only β -amino acid chosen without additional functional groups off of the aryl ring was 3-amino-3-(3-((3,4,5-trihydroxybenzoyl)oxy)phenyl)propanoic acid (Fig. 5). This β -amino acid was also only one of two that had a meta relationship to amino acid motif while the other five had a para relationship. In common with 3-amino-3-(3-methoxy-4-((3,4,5-trihydroxybenzoyl)oxy)phenyl)propanoic acid this molecule had the same interactions through the amino acid group utilizing residues Asp129, Arg18, Cys17 and Ile16 in the same fashion for hydrogen bonding. It was interesting to note that all β -amino acids hydrogen bonded with the aforementioned residues. Also, π - π non-polar interactions were seen for all β -amino acids and Tyr131. These interactions may be important for tight binding to LMW-PTP IF2 suggested by

their better docking scores than PLP and NSC107022. All of the β -amino acids entered the active site with amino acid motif with the galloyl group pointing out of the active site and can be seen docked in LMW-PTP IF2 with key interactions in figures 5-11.

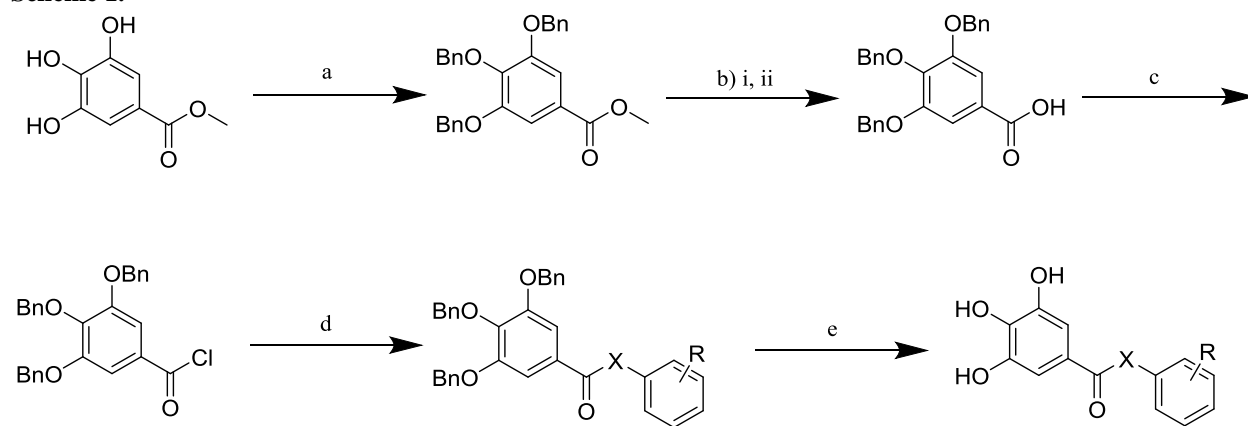
The screening of primary aromatic amines utilizing an amide linkage with the galloyl base resulted in poorer docking scores than the esters, NSC107022 and PLP. While the docking scores for LMW-PTP IF2 were not better than PLP, the docking scores in LMW-PTP IF1 were higher than PLP which suggests poor binding into this isoform which is a desirable quality for useful inhibitors. A potential cause for these resultant docking scores may be the restricted rotation about the amide bond compared to an ester bond. Nonetheless, four amide inhibitors were chosen to be synthesized based off docking score and ease of synthesis. The top amide inhibitor was 3-(3,4,5-trihydroxybenzamido)phthalic acid (-7.434) which was near that of PLP. This amide utilized Asp129 for hydrogen bonding as did the β -amino acids and NSC107022; however, the hydrogen bonds were through the hydroxyl groups of the galloyl base (Fig. 14). 3-(3,4,5-trihydroxybenzamido)phthalic acid also had π - π interactions with Tyr132 and the aromatic ring of the galloyl base. The hydroxyl group of the meta carboxylic acid hydrogen bonded to Trp49 and Arg53 while the ortho carboxylic group showed no significant interactions. 2-Nitro-5-(3,4,5-trihydroxybenzamido)benzoic acid was oriented in the active site of LMW-PTP IF2 in a similar fashion to 3-(3,4,5-trihydroxybenzamido)phthalic acid. Hydrogen bonding was once again seen between Asp129 and the two of the galloyl hydroxyl group. Tyr132 also showed an interaction; however, this was a hydrogen bond to the last hydroxyl group of the galloyl base rather than a π - π interaction (Fig. 15). The remaining two amide inhibitors were not bound to LMW-PTP IF2 similarly to the previous two amides of β -amino acids (Figs. 11 and 12). 2-(4-(3,4,5-trihydroxybenzamido)phenethyl)-1,4-phenylene diacetate did utilize Asp129 for hydrogen bonding through the nitrogen of the amide and one of the galloyl hydroxyl groups (Fig. 12).

3-Hydroxyphenyl 3,4,5-trihydroxybenzoate was the sole inhibitor chosen to be synthesized before *in silico* screening took place. This molecule was chosen based on its similarity to NSC107022 along with the added degrees of freedom. This was thought to give the inhibitor more freedom to situate itself in the active site; however, docking into LMW-PTP IF2 resulted in a poor docking score (-6.276). Once again Asp129 and Tyr132 hydrogen bonded with the hydroxyl groups of the galloyl base as well as π - π interactions with the galloyl ring and Tyr132 (Fig. 4). Asp129 was utilized by all inhibitors to form hydrogen bonds with LMW-PTP

IF2 and suggests it is an important residue in the inhibition of the enzyme. The amide inhibitors lacked interaction with Arg18 which was seen in all β -amino acid ester inhibitors, NSC107022 and PLP. The poorer docking scores seen for the amide inhibitors may be due to the lacking of this interaction and also points to its importance in inhibition of LMW-PTP IF2. The added interactions of Cys17 and Ile16 for hydrogen bonding and Tyr131 for π - π interactions seen in the β -amino acid ester inhibitors suggests interaction with these residues result in tighter binding to LMW-PTP IF2. Structures and docking scores in LMW-PTP IF2 and IF1 for all chosen inhibitors can be seen in Table 1.

Original synthesis of the galloyl inhibitors involved the conversion of gallic acid to its acid chloride derivative and immediate coupling to either the aryl alcohol or aromatic amine. This resulted in the unwanted coupling between galloyl groups and was abandoned as a viable synthetic route. Starting from methyl gallate, synthesis of galloyl ester and amide inhibitors could be achieved in five steps with the exception of an extra step to prepare the β -amino acid coupling partners as adapted from previous literature and seen in Scheme 1.¹⁵ Following this

Scheme 1.

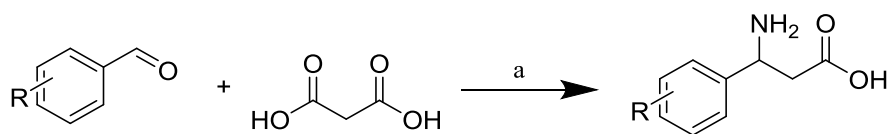


Reagents and conditions. BnBr, K_2CO_3 , KI, acetone, reflux b) i. 6.0 M NaOH, reagent alcohol, reflux, ii. 0.6 M HCl, rt c) $(COCl)_2$, toluene, 70°C d) aryl alcohol/aromatic amine, DMAP, CH_3CN , rt or reflux e) H_2 atmosphere, toluene, 40°C, X=O or NH.

route, 3-hydroxyphenyl 3,4,5-trihydroxybenzoate was successfully synthesized which proved this to be a useful path towards synthesis of galloyl ester and amide inhibitors. 3-Hydroxyphenyl 3,4,5-trihydroxybenzoate was then assayed *in vitro* and fit to a competitive inhibition model to find its inhibition constant ($K_i \gg 500 \mu M$). This first fully synthesized inhibitor showed very little inhibition in LMW-PTP IF2. Before synthesis of galloyl esters could continue the β -amino

acid coupling partners had to be prepared from their aldehyde derivative. The β -amino acid motif has become more common in pharmaceutical products for its stability against protease hydrolysis and presence in many natural products.^{16,17} For this reason facile one-pot synthesis of β -amino acid derivatives have been developed.^{17,18} The synthetic route is outlined in Scheme 2. 3-Amino-3-(3-hydroxyphenyl)propanoic acid was successfully synthesized following this route; however, the remaining β -amino acids were not able to be prepared. Presence of the hydroxyl group in the para position proved to donate electron density towards the aldehyde which reduced its electrophilicity nature and made it unable to participate in the desired reaction. Electron withdrawing groups, such as a simple acetate group and a trifluoro acetate group, were placed on

Scheme 2.



Reagents and conditions. a) NH_4OAc , EtOH, reflux.

the hydroxyl group to pull electron density away from the aldehyde. The presence of these groups did not result in successful synthesis of the β -amino acids due to the esters being cleaved under the given conditions resulting in a phenoxy anion. Literature reported products did not have strong electron donating groups in the para position^{17,18} and to the best of our knowledge only one β -amino acid with a hydroxyl group in the para position has been reported.¹⁹ To test if an electron withdrawing group in the para position could promote β -amino acid formation we started with 4-nitrobenzaldehyde and followed the conditions outlined in Scheme 2. This proved to be a successful route to synthesis the β -amino acids. Furthermore, to show that a phenoxy anion shuts down the reaction we started with 4-anisaldehyde and followed Scheme 2. The methoxy group proved to block phenoxy anion formation and resulted in the β -amino acid. This leads us to believe future β -amino acids with a hydroxyl group in the para position could be synthesized through protection of the hydroxyl group with tert-butyldimethylsilyl ether (TBDMS), which is stable under the given conditions, and later cleaved under mild conditions to yield the final β -amino acid. Both synthetic strategies proved successful and will allow us to form the desired β -amino acids followed by conversion of the nitro or TBDMS group to the necessary hydroxyl or amine group to yield the final β -amino acid coupling partner. Galloyl amide inhibitors were then prepared following Scheme 1. Two of the four chosen galloyl amide

inhibitors have been crudely synthesized but have not been purified and hydrogenated to yield final inhibitors for *in vitro* evaluation.

Conclusion

The *in silico* screening of galloyl ester and amide inhibitors for human LMW-PTP IF2 yielded 11 compounds for synthesis, seven esters and four amides, along with one ester prior to *in silico* screening. Asp129 was utilized by most inhibitors along with NSC107022 and PLP which suggests its importance in inhibition of LMW-PTP IF2. Arg18 was also seen interacting with all galloyl ester inhibitors, NSC107022 and PLP; however, this interaction was not seen in galloyl amide inhibitors which may have resulted in the poorer docking scores for the amides. Additional interactions with Cys17, Ile16 and Tyr131 seen in the β -amino acid motif of galloyl ester inhibitors may be important sites of intermolecular bonding which results in tighter binding to LMW-PTP IF2. The only fully synthesized inhibitor, 3-hydroxyphenyl 3,4,5-trihydroxybenzoate, showed very little inhibition of LMW-PTP IF2 when assayed *in vitro*.

Further synthesis of galloyl amide inhibitors as well as a better process for synthesis of β -amino acid coupling partners will result in more potential inhibitors of LMW-PTP IF2 and further optimization of NSC107022. Also, *in vitro* screening against LMW-PTP IF1 will determine inhibitor specificity for the two active isoforms of LMW-PTP and lead to new, specific inhibitors of LWM-PTP IF2.

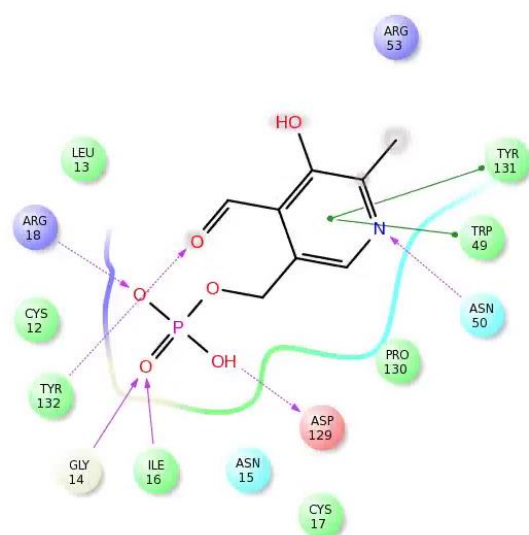


Fig. 2. PLP docked in LMW-PTP IF2 with key interactions shown.

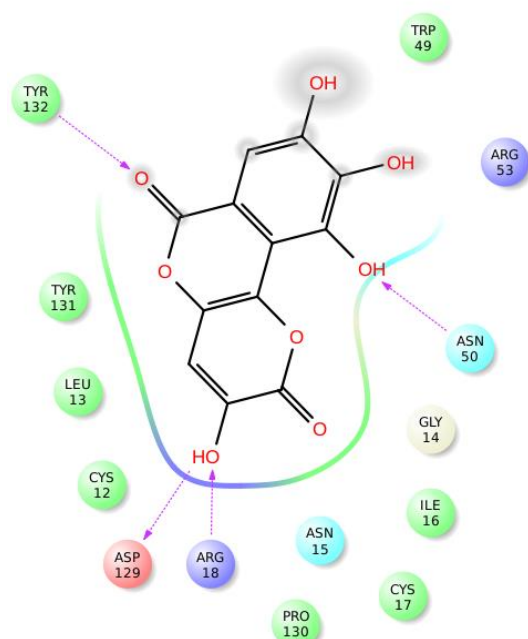


Fig. 3. Residue interactions of NSC107022 docked in LMW-PTP IF2.

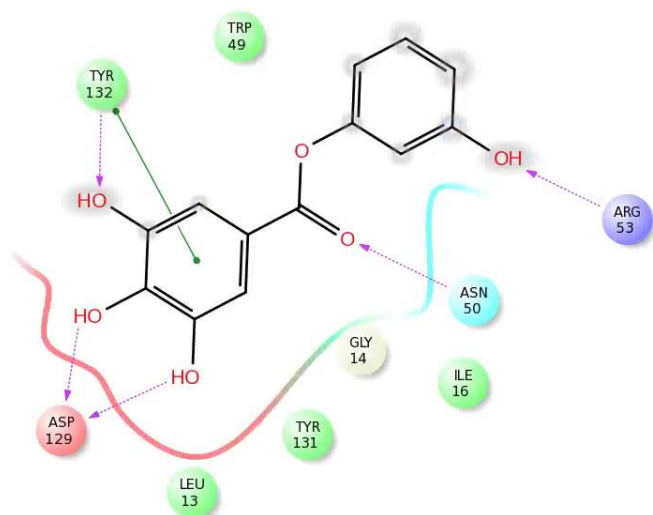


Fig. 4. 3-hydroxyphenyl 3,4,5-trihydroxybenzoate docked in LMW-PTP IF2 with key residue interactions shown.

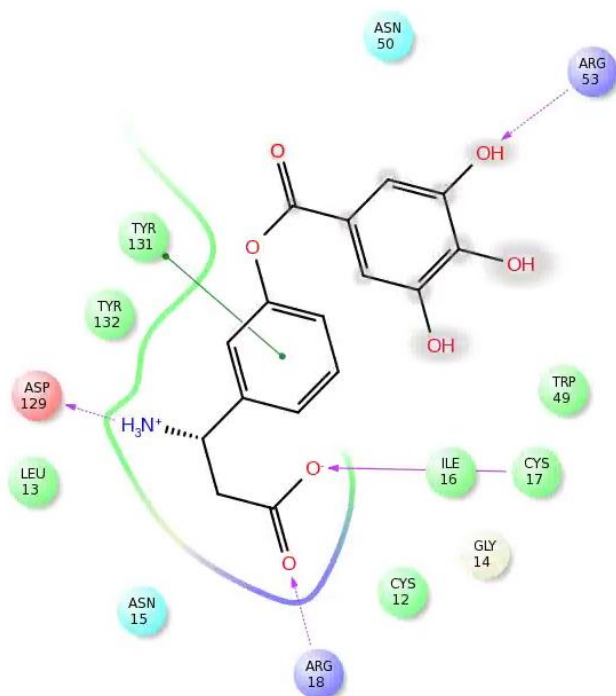


Fig. 5. 3-amino-3-(3-((3,4,5-trihydroxybenzoyl)oxy)phenyl)propanoic acid docked in LMW-PTP IF2 with key interactions shown.

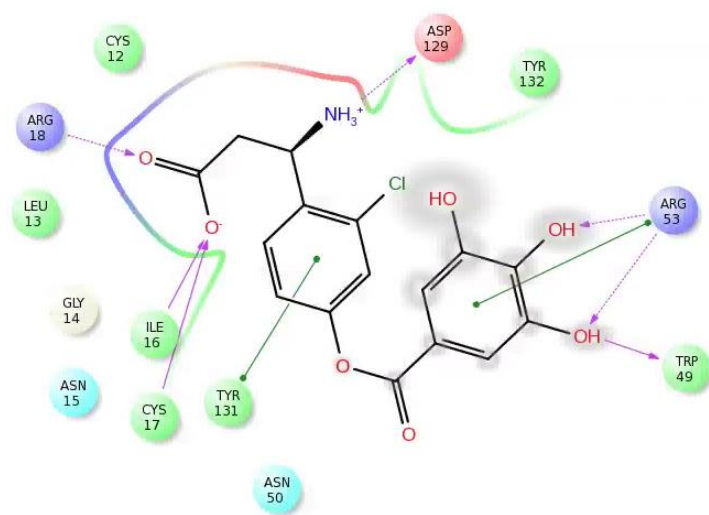


Fig. 6. 3-amino-3-(2-chloro-4-((3,4,5-trihydroxybenzoyl)oxy)phenyl)propanoic acid docked in LMW-PTP IF2 with key interactions shown.

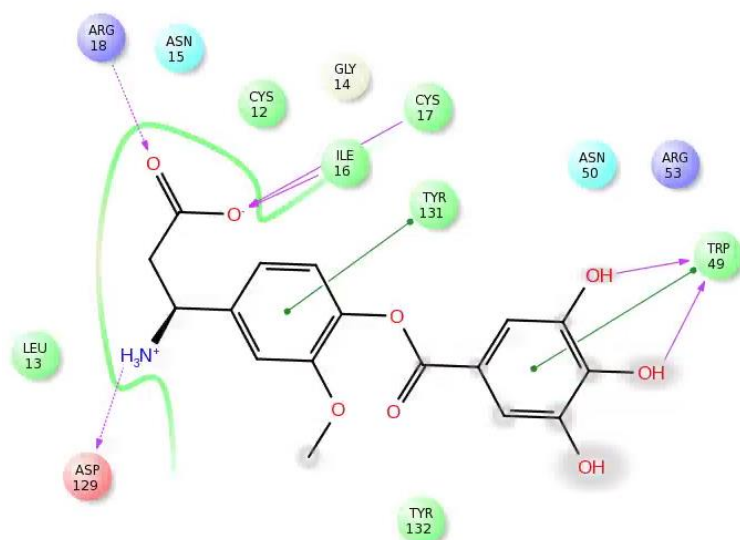


Fig. 7. 3-amino-3-(3-methoxy-4-((3,4,5-trihydroxybenzoyl)oxy)phenyl)propanoic acid docked in LMW-PTP IF2 with key interactions shown.

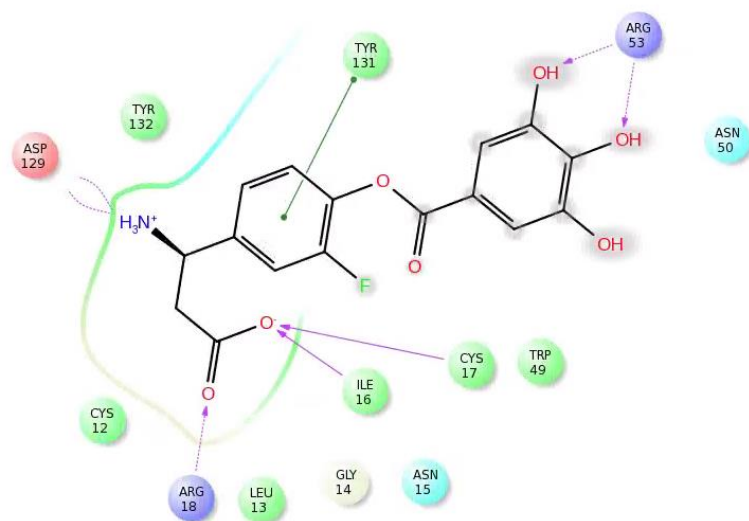


Fig. 8. 3-amino-3-(3-fluoro-4-((3,4,5-trihydroxybenzoyl)oxy)phenyl)propanoic acid docked in LMW-PTP IF2 with key interactions shown.

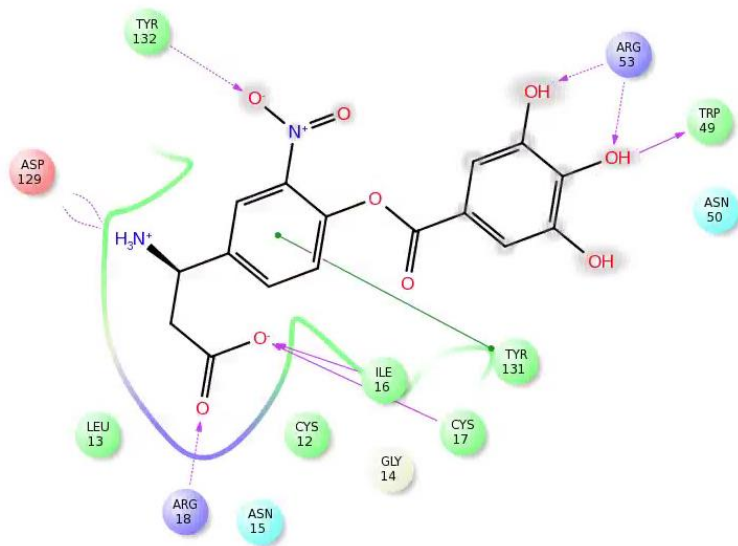


Fig. 9. 3-amino-3-(3-nitro-4-((3,4,5-trihydroxybenzoyl)oxy)phenyl)propanoic acid docked in LMW-PTP IF2 with key interactions shown.

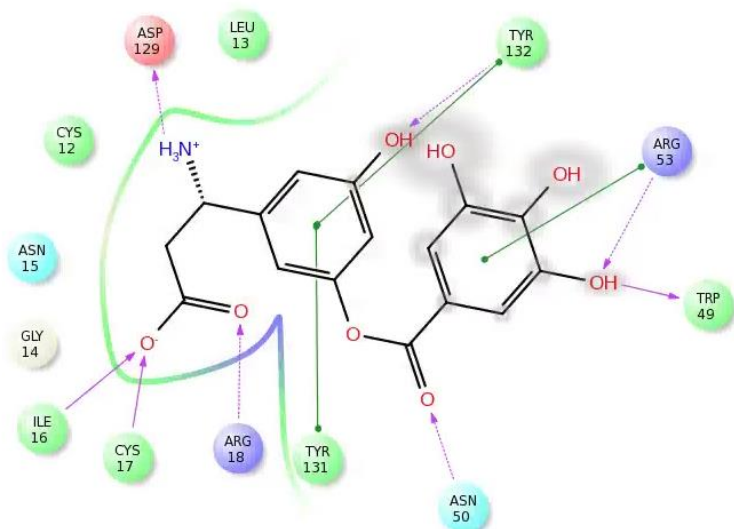


Fig. 10. 3-amino-3-(3-hydroxy-5-((3,4,5-trihydroxybenzoyl)oxy)phenyl)propanoic acid docked in LMW-PTP IF2 with key interactions shown.

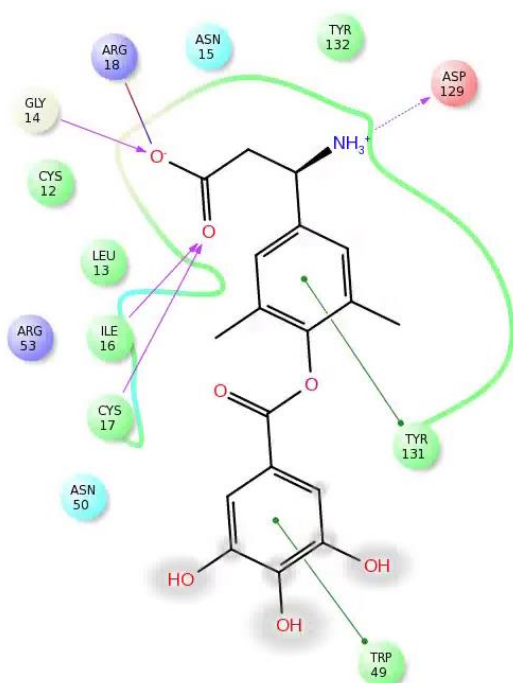


Fig. 11. 3-amino-3-(3,5-dimethyl-4-((3,4,5-trihydroxybenzoyl)oxy)phenyl)propanoic acid docked in LMW-PTP IF2 with key interactions shown.

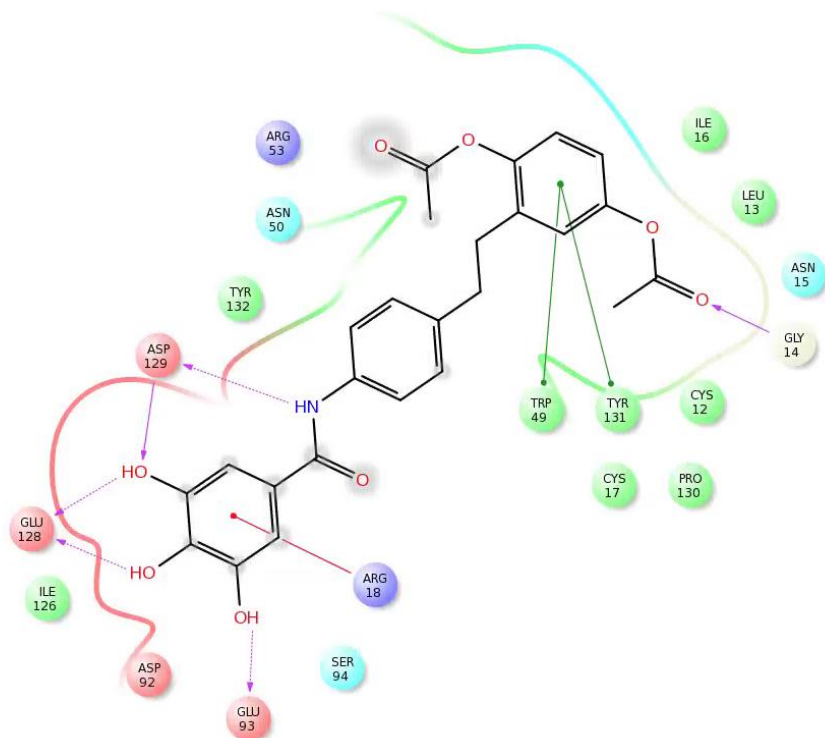


Fig. 12. 2-(4-(3,4,5-trihydroxybenzamido)phenethyl)-1,4-phenylene diacetate docked in LMW-PTP IF2 with key interactions shown.

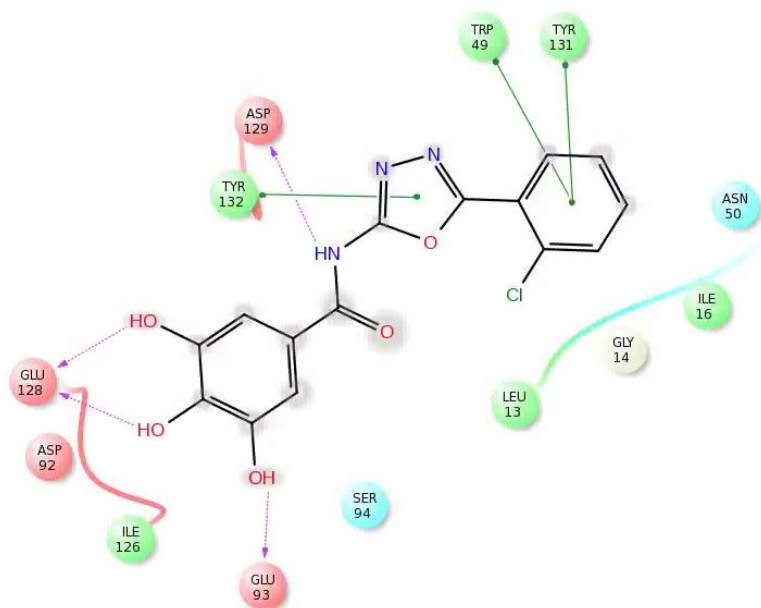


Fig. 13. N-(5-(2-chlorophenyl)-1,3,4-oxadiazol-2-yl)-3,4,5-trihydroxybenzamide docked in LMW-PTP IF2 with key interactions shown.

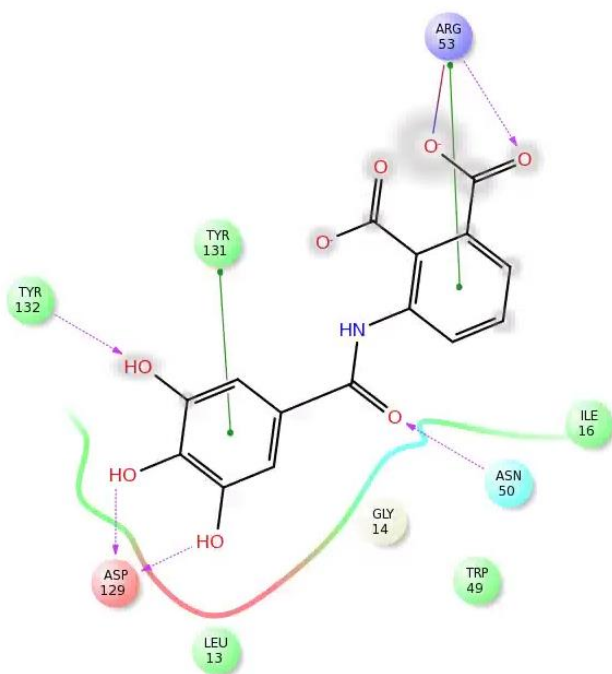


Fig. 14. 3-(3,4,5-trihydroxybenzamido)phthalic acid docked in LMW-PTP IF2 with key interactions shown.

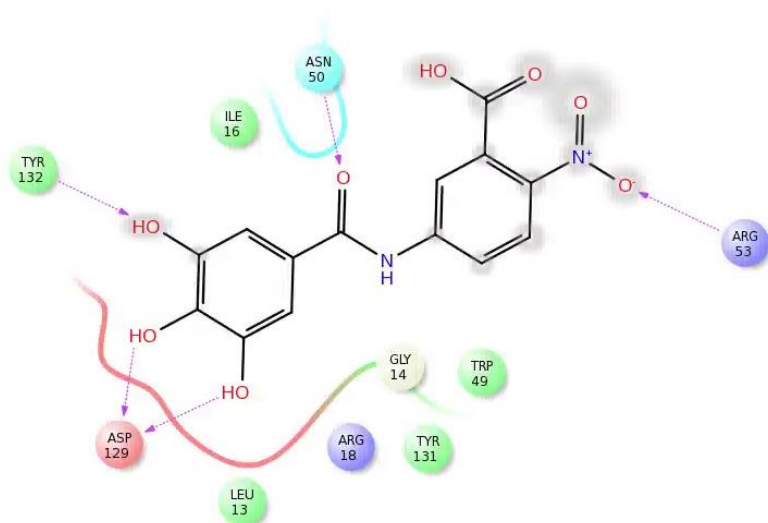
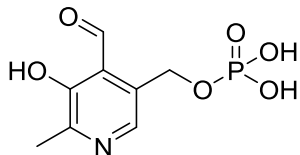
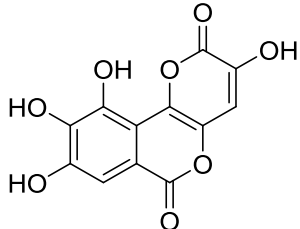
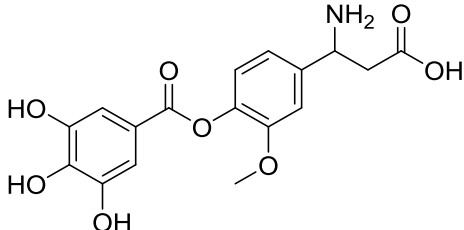
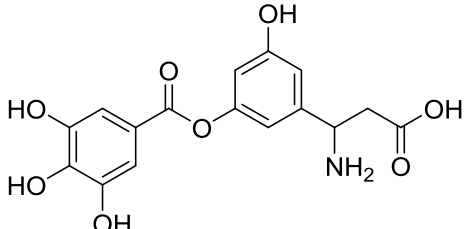
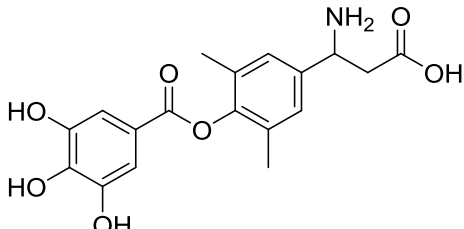
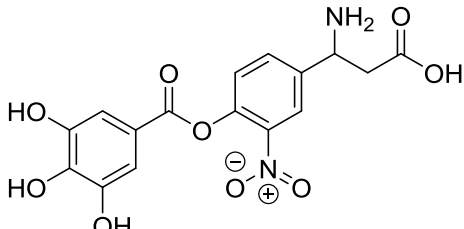
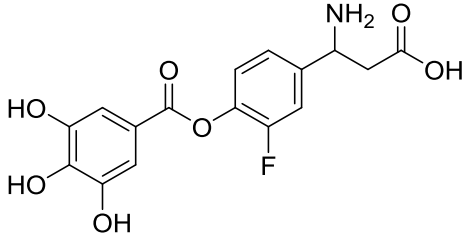
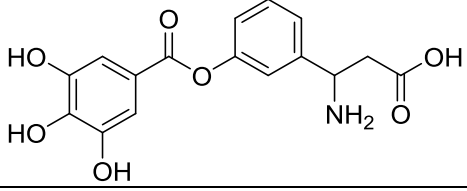
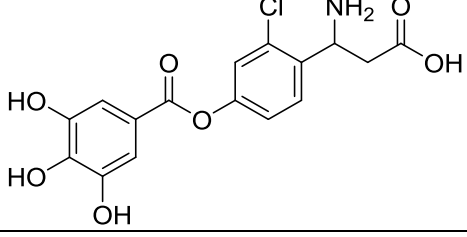
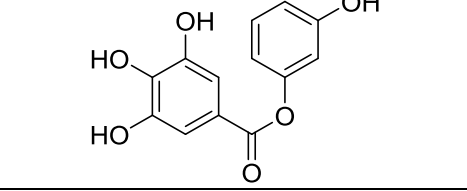
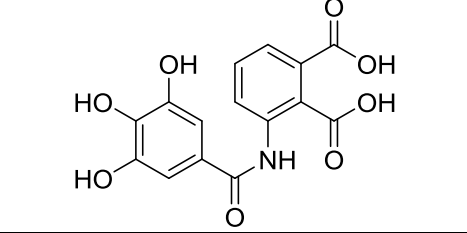
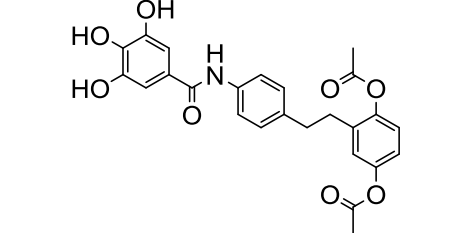
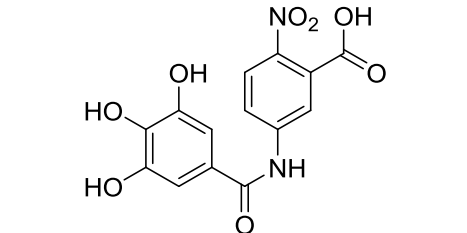
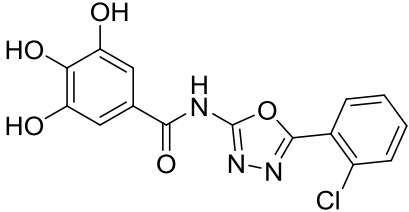


Fig. 15. 2-nitro-5-(3,4,5-trihydroxybenzamido)benzoic acid docked in LMW-PTP IF2 with key interactions shown.

Table 1. Inhibitors structures and docking scores in LMW-PTP IF2 and IF1 along with PLP and NSC107022. Docking scores for NSC107022 obtained from Seiler *et al.*

| Molecule | LMW-PTP IF2 | LWM-PTP IF1 |
|---|-------------|-------------|
|  | -8.158 | -7.625 |
|  | -8.787 | -5.743 |
|  | -10.401 | -11.343 |
|  | -10.332 | -9.108 |
|  | -9.826 | -6.292 |
|  | -9.790 | -8.600 |

| | | |
|--|--------|--------|
|  <chem>NC(=O)CCc1ccc(cc1)OC(=O)c2cc(O)c(O)c(O)c2</chem> | -9.667 | -8.543 |
|  <chem>NC(=O)Cc1ccc(cc1)OC(=O)c2cc(O)c(O)c(O)c2</chem> | -9.538 | -8.383 |
|  <chem>NC(=O)CCc1ccc(Cl)cc1OC(=O)c2cc(O)c(O)c(O)c2</chem> | -9.397 | -7.456 |
|  <chem>Oc1ccc(cc1)OC(=O)c2cc(O)c(O)c(O)c2</chem> | -6.276 | -6.069 |
|  <chem>O=C(Nc1cc(O)c(O)c(O)c1)C(=O)Oc2cc(O)c(O)c(O)c2</chem> | -7.434 | -6.022 |
|  <chem>CC(=O)Oc1cc(OC(=O)C)cc(OC(=O)C)c1Cc2ccc(NC(=O)c3cc(O)c(O)c(O)c3)cc2</chem> | -6.065 | -3.435 |
|  <chem>O=C(Nc1ccc(cc1)C(=O)O[N+](=O)[O-])C(=O)c2cc(O)c(O)c(O)c2</chem> | -5.568 | -5.992 |

| | | |
|---|--------|--------|
|  | -5.258 | -4.621 |
|---|--------|--------|

Experimental

Methyl 3,4,5-tribenzyloxybenzoate. A mixture of 186 mg (1 mmol) methyl 3,4,5-trihydroxybenzoate, 795 mg (5.75 mmol) potassium carbonate and 33 mg (0.2 mmol) potassium iodide in 15 mL of dry acetone was stirred at room temperature for 20 min. At this time 380 μ L (3.2 mmol) benzyl bromide in 1 mL of dry acetone was slowly added. The mixture was then heated to reflux for 18 h. At this time the reaction mixture was filtered, and the filtrate was evaporated to dryness then further dried under vacuum for 1 h to yield 425 mg (94%) 3,4,5-tribenzyloxybenzoate as a white solid. ^1H NMR (CD_3COCD_3) δ 3.83 (3H, s), 5.11 (2H, s), 5.20 (4H, s) 7.25-7.50 (17H, m).

3,4,5-Tribenzyloxybenzoic acid. 107 mg (0.24 mmol) methyl 3,4,5-tribenzyloxybenzoate was suspended in 10 mL reagent alcohol. 60 μ L (0.35 mmol) 6M sodium hydroxide was added and mixture was heated to reflux for 2 h. The reaction mixture was then poured into 10 mL of hot 0.6M hydrogen chloride and a white precipitate immediately forms which was stirred for 10 min. The precipitate was then filtered and washed successively with 2 mL 1:1 reagent alcohol/ H_2O , 2 mL H_2O , 2 mL reagent alcohol, 2x1 mL methanol and 2x1 mL TBME. Resulting solid was then dried under vacuum for 3 h to yield 95 mg (91%) 3,4,5-tribenzyloxybenzoic acid as a white solid. ^1H NMR (CD_3COCD_3) δ 5.11 (2H, s), 5.21 (4H, s), 7.24-7.50 (17H, m).

3,4,5-Tribenzyloxybenzoyl chloride. 73 mg (0.17 mmol) 3,4,5-tribenzyloxybenzoic acid was suspended in 3 mL toluene and stirred at room temperature. 30 μ L (0.33 mmol) oxalyl chloride in 1 mL toluene was added dropwise over 5 min and stirring at room temperature continued for 20 min. The reaction mixture was then heated to 50 $^\circ\text{C}$ for 1 h. The mixture was then concentrated and taken up in 3 mL of toluene at 70 $^\circ\text{C}$ and added to 3 mL cold cyclohexane. No precipitate was formed so the solution was evaporated to dryness and dried under vacuum for 1 h.

to yield 76 mg (97%) 3,4,5-tribenzyloxybenzoyl chloride as a light yellow solid. ^1H NMR (CD_3COCD_3) δ 5.20 (2H, s), 5.26 (4H, s), 7.26-7.51 (17H, s).

3-Hydroxyphenyl 3,4,5-tribenzyloxybenzoate. 65 mg (0.14 mmol) 3,4,5-tribenzyloxybenzoyl chloride, 65 mg (0.59 mmol) resorcinol and 16 mg (0.13 mmol) 4-dimethylaminopyridine were suspended in 3 mL acetonitrile and stirred at room temperature for 18 h. The reaction mixture was evaporated to dryness and purified on a silica column eluting with 65:35 hexanes/ethyl acetate to yield 33 mg (44%) 3-hydroxyphenyl 3,4,5-tribenzyloxybenzoate as a white solid. ^1H NMR (CD_3COCD_3) δ 5.16 (2H, s), 5.25 (4H, s), 6.28 (1H, m), 6.71 (2H, m) 7.26-7.56 (18H, m), 8.65 (1H, s).

3-Hydroxyphenyl 3,4,5-trihydroxybenzoate. A suspension of 86 mg (0.16 mmol) 3-hydroxyphenyl 3,4,5-tribenzyloxybenzoate and 38 mg (0.36 mmol) Pd/C was suspended in dry THF and stirred at 40°C under a positive atmosphere of hydrogen for 16 h. The reaction mixture was then cooled to room temperature and filtered through a thin layer of celite. The filtrate was evaporated to dryness and dried under a vacuum for 2 h to yield 40 mg (95%) 3-hydroxyphenyl 3,4,5-trihydroxybenzoate as a gray semisolid. ^1H NMR (CD_3COCD_3) δ 6.29 (1H, m), 6.69-6.75 (2H, m), 7.22-7.24 (3H, m), 8.22 (1H, s) 8.39 (2H, s), 8.6 (1H, s).

3-Amino-3-(3-hydroxyphenyl)propanoic acid. A mixture of 247 mg (2 mmol) 3-hydroxybenzaldehyde and 313 mg (3 mmol) ammonium acetate in 5 mL ethanol was heated to reflux and stirred for 1 h. At this time 310 mg (4 mmol) malonic acid and an additional equivalent of ammonium acetate were added and refluxing continued for 3 h. A white precipitate formed in the reaction flask and was allowed to cool to room temperature before being placed on ice for one half hour. The precipitate was then filtered, washed with 2 x 1 mL ethanol and dried under reduced pressure for 1 h to yield 133 mg (37%) 3-amino-3-(3-hydroxyphenyl)propanoic acid as a white solid. ^1H NMR (D_2O) δ 2.63-2.75 (2H, m), 4.45 (1H, t), 6.78 (1H, m), 6.86 (2H, m), 7.24 (1H, M).

3-Amino-3-(4-nitrophenyl)propanoic acid. A mixture of 100 mg (0.7 mmol) 4-nitrobenzaldehyde, 91 mg (0.88 mmol) malonic acid and 108 mg (1.4 mmol) ammonium acetate

in 5 mL ethanol was heated to reflux and stirred for 18 h. An off-white precipitate formed and was filtered and washed with 2 x 1 mL cool ethanol. The solid was collected and dried under reduced pressure to yield 60 mg (40%) 3-amino-3-(4-nitrophenyl)propanoic acid as an off-white solid. ^1H NMR (D_2O) δ 2.73-2.86 (2H, m), 4.67 (1H, t), 7.63 (2H, d), 8.11 (2H, d).

3-Amino-3-(4-methoxyphenyl)propanoic acid. A mixture of 95 mg (0.7 mmol) 4-anisaldehyde, 91 mg (0.875 mmol) malonic acid and 108 mg (1.4 mmol) ammonium acetate in 5 mL ethanol was heated to reflux and stirred for 18 h. A white precipitate formed and was filtered. Subsequent 2 x 1 mL washings with cool ethanol and drying under reduced pressure yielded 3-amino-3-(4-methoxyphenyl)propanoic acid as a white solid. Yield was not recorded. ^1H NMR (D_2O) δ 2.65-2.88 (2H, m), 3.74 (3H, s), 4.52 (1H, t), 6.96 (2H, d), 7.30 (2H, d).

Supporting Information Experimental procedures for *in silico* methods and *in vitro* assay along with ^1H NMR spectra for synthesized compounds can be found in the supporting information.

Acknowledgements The authors would like to thank the Minnesota Supercomputing Institute for the use of their resources for *in silico* work and Steve Gradin from the CSB/SJU IT Services for help connecting to MSI remotely. We also acknowledge the CSB/SJU Chemistry department, the CSB/SJU Undergraduate Research Program, the Honors Thesis Summer Fellowship and the Rooney Grant for their support throughout the duration of this work.

References

1. Maccari, R.; Ottaná, R. Low Molecular Weight Phosphotyrosine Protein Phosphatase as Emerging Targets for the Design of Novel Therapeutic Agents. *J. Med. Chem.* **2012**, *55*, 2-22.
2. Souza, A. C.; Azoubel, S.; Queiroz, K.C.; Peppelenbosch, M. P.; Ferreira, C. V. From immune response to cancer: a spot on the low molecular weight protein tyrosine phosphatase. *Cell Mol. Life Sci.* **2009**, *66*, 1140-1153.
3. Raugei, G.; Rampone, G.; Chiarugi, P. Low molecular weight protein tyrosine phosphatases: small, but smart. *Cell Mol. Life Sci.* **2002**, *59*, 941-949.
4. Seiler, C. L.; Richards, K. A.; Jakubowski, H. V.; McIntee, E. J. Identification of new inhibitors for low molecular weight protein tyrosine phosphatase isoform B. *Bioorg. Med. Chem. Lett.* **2013**, *23*, 5912-5914.
5. Kikawa, K. D.; Vidale, D. R.; Van Etten, R. L.; Kinch, M. S. Regulation of the EphA2 kinase by the low molecular weight tyrosine phosphatase induces transformation. *J. Biol. Chem.* **2002**, *277*, 39274-39279.

6. Chiarugi, P.; Taddei, M. L.; Schiavone, N.; Papucci, L.; Giannoni, E.; Fiaschi, T.; Capaccioli, S.; Taugei, G. LMW-PTP is a positive regulator of tumor onset and growth. *Oncogene*. **2004**, *23*, 3905-3914.
7. Marzocchi, R.; Malentacchi, F.; Biagini, M.; Cirelli, D.; Luceri, C.; Caderni, G.; Raugei, G. The expression of low molecular weight protein tyrosine phosphatase is up-regulated in 1,2-dimethylhydrazine-induced colon tumours in rats. *Int. J. Cancer*. **2008**, *122*, 1675-1678.
8. Malentacchi, F.; Marzocchi, R.; Gelmini, S.; Orlando, C.; Serio, M.; Ramponi, G.; Raugei, G. Up-Regulated Expression of Low Molecular Weight Protein Tyrosine Phosphatases in Different Human Cancers. *Biochem. Biophys. Res. Commun.* **2005**, *334*, 875-883.
9. Homan, K. T.; Balasubramaniam, D.; Zabell, A. P.; Wiest, O.; Helquist, P.; Stauffacher, C. V. Identification of novel inhibitors for a low molecular weight protein tyrosine phosphatase via virtual screening. *Bioorg. Med. Chem.* **2010**, *18*, 5449-5456.
10. Miao, H.; Li, D.; Mukherjee, A.; Guo, H.; Petty, A.; Cutter, J.; Basilion, J. P.; Sedor, J.; Wu, J.; Danielpour, D.; Sloan, A. E.; Cohen, M. L.; Wang, B. EphA2 Mediates Ligand-Dependent Inhibition and Ligand-Independent Promotion of Cell Migration and Invasion via a Reciprocal Regulatory Loop with Akt. *Cancer Cell*. **2009**, *16*, 9-20.
11. Zhang, M.; Stauffacher, C. V.; Lin, D.; Van Etten, R. L.; Crystal Structure of a Human Low Molecular Weight Phosphotyrosyl Phosphatase. Implications for Substrate Specificity. *J. Biol. Chem.* **1998**, *262*, 21714-21720.
12. Cirri, P.; Fiaschi, T.; Chiarugi, P.; Camici, G.; Manao, G.; Raugei, G.; Ramponi, G. The Molecular Basis of the Different Kinetic Behavior of the Two Low Molecular Mass Phosphotyrosine Protein Phosphatase Isoforms. *J. Biol. Chem.* **1996**, *271*, 2604-2607.
13. Alho, I.; Costa, L.; Bicho, M.; Coelho, C. Characterization of Low Molecular Weight Protein Tyrosine Phosphatase Isoforms in Human Breast Cancer Epithelial Cell Lines. *Anticancer Res.* **2013**, *33*, 1983-1988.
14. Zhou, M.; Van Etten, R. L. Structural Basis of the Tight Binding of Pyridoxal 5'-Phosphate to a Low Molecular Weight Protein Tyrosine Phosphatase. *Biochem.* **1999**, *38*, 2636-2646.
15. Ren, Y.; Himmeldirk, K.; Chen, X. Synthesis and Structure—Activity Relationship Study of Antidiabetic Penta-*O*-galloyl-D-Glucopyranose and Its Analogues. *J. Med. Chem.* **2006**, *49*, 2829-2837.
16. Seebach, D.; Beck, A. K.; Bierbaum, D. J. The World of β - and γ -Peptides Comprised of Homologated Proteinogenic Amino Acids and Other Components. *Chem. Biodiversity*. **2004**, *1*, 1111-1239.
17. Grayson, J. I.; Roos, J.; Osswald, S. Development of a Commercial Process for (S)- β -Phenylalanine. *Org. Process Res. Dev.* **2011**, *15*, 1201-1206.
18. Tan, C. Y. K.; Weaver, D. F. A one-pot synthesis of 2-amino-3-arylpropionic acids. *Tetrahedron*. **2002**, *58*, 7449-7461.
19. Ru, J.; Hui, C.; Si-Kun, C.; Ying, J.; Qiao-Feng, W.; Xiao-Li, S. Improved one-pot synthesis of 3-amino-3-arylpropionic acids. *J. Fourth Mil. Med. Univ.* **2004**, *25*, 688-691.

Supporting Information

Molecular Modeling:

Combinatorial Screening: A library of aromatic alcohols (approx. 3000 compounds) and the primary aromatic amine Selected Structure Set (approx. 3500 compounds) were obtained from Aldrich and were linked to the galloyl core for *in silico* screening using Maestro (Schrodinger, LLC.). 3,4,5-Tribenzyloxybenzoyl chloride was drawn and incorporated into Maestro workspace to be used as the coupling core. The core was then minimized and prepared using LigPrep with the MMFFs force field and a target pH of 5.5 ± 2.0 . Compound libraries were then broken into smaller subsets and prepared using Reagent Preparation with the same target pH. The Amine_Primary_N_H functional group was selected and set to generate at most 10 stereoisomers per compounds. Reagent prepared libraries and the galloyl core were then combined and docked into the 1XWW grid that was previously prepared using the Combinatorial Screening feature of Maestro. Once complete, compounds were analyzed and selected based on docking score with a more negative score being a better inhibitor.

Individual Docking: After completion of combinatorial screening the top molecules were chosen based on docking score and ease of synthesis. These molecules were then docked individually into LMW-PTP IFB and IFA (1XWW and 5PNT, respectively) using the Glide docking feature of Maestro. The molecules were first drawn and incorporated into the Maestro work space. Minimization and ligand preparation were carried out as previously described. Once prepared the molecules were docked into either the 1XWW or 5PNT grids that were previously prepared using extra precision (XP) and flexible ligand sampling with the addition of Epik state penalties. The number of poses to report was set to 10 and performance of post-docking minimization was selected. Residue interaction scores were set for residues within 12.0 Å of the grid center.

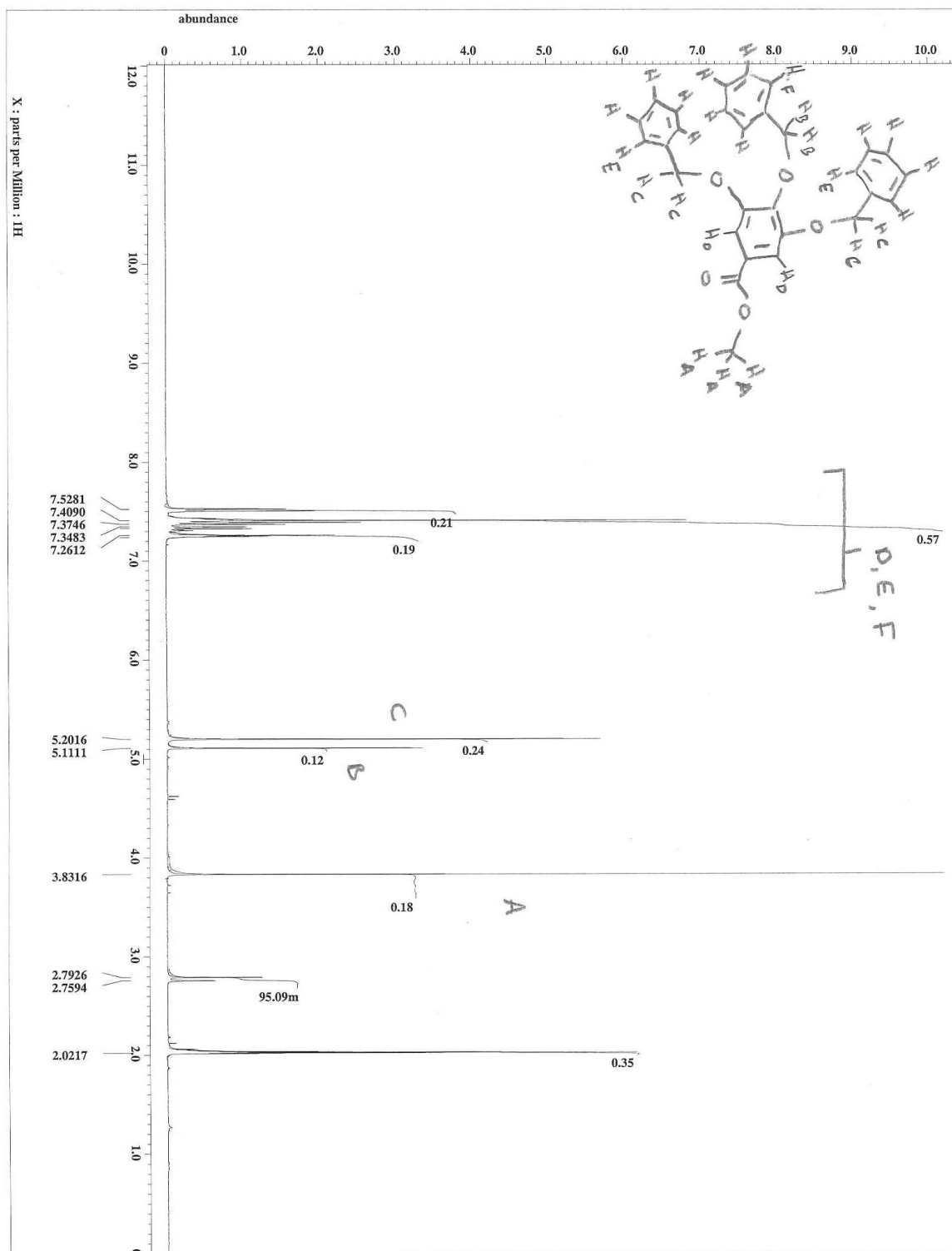
In vitro assay:

Solution preparation: A 1.0 M acetic acid/sodium acetate buffer at pH 5.5 was prepared by dissolving 13.6 g sodium acetate in 100 mL of E-pure H₂O and adding enough 1.0 M acetic acid (5.75 mL glacial acetic acid/100 mL E-pure H₂O) to adjust the pH to desired value (approx. 15 mL). 2.8 g of solid sodium hydroxide was added to 100 mL E-pure H₂O to create a 0.5 sodium

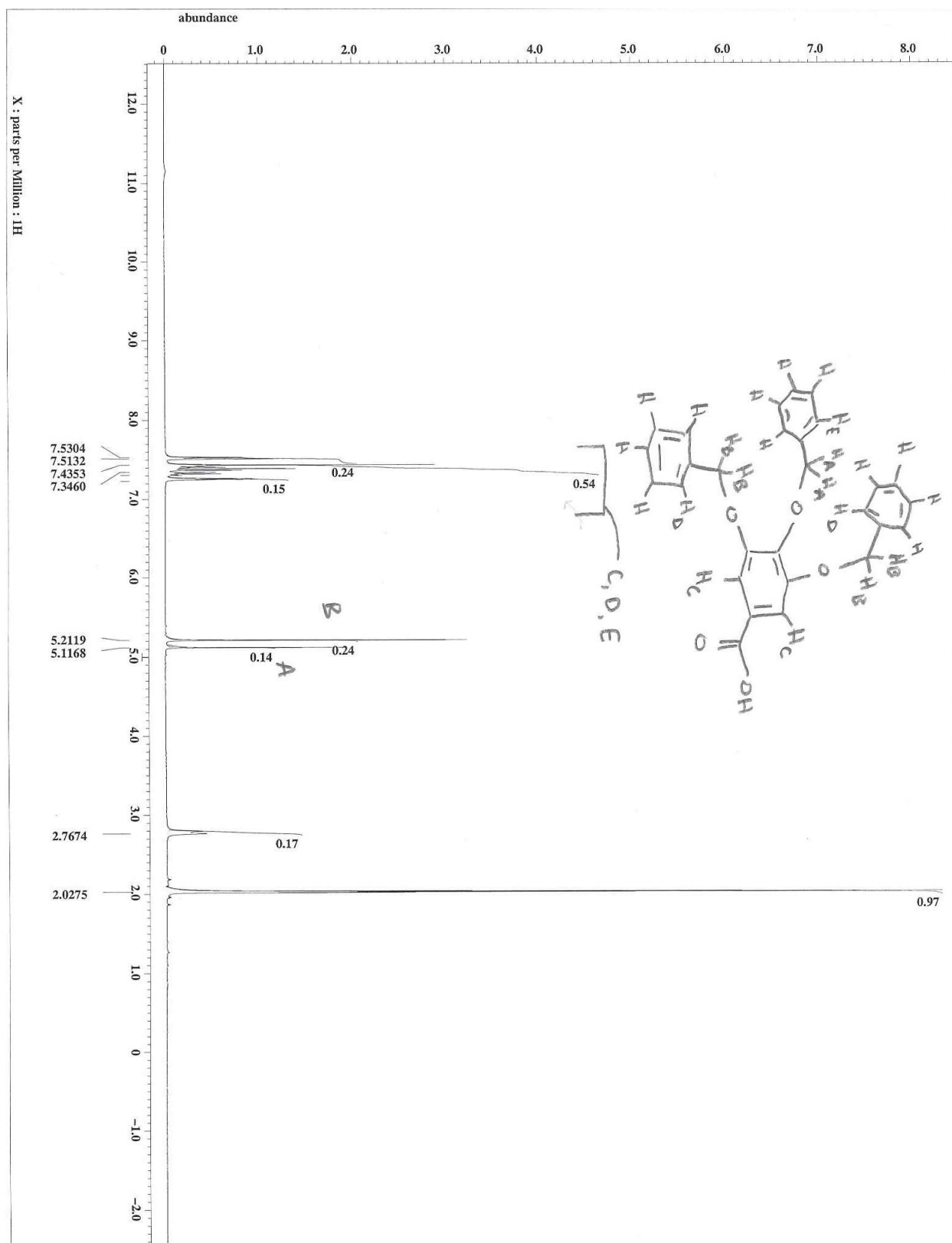
hydroxide solution used to quench the enzymatic reaction. P-nitrophenyl phosphate (pnpp) substrate was prepared as a stock 50 mM solution through the dissolving of 0.932 g of pnpp in 50 mL E-pure H₂O. The stock solution was diluted to sub-stock solutions of 10.0 mM, 5.0 mM, 2.5 mM, 1.25 mM, 0.80 mM, 0.625 mM, 0.50 mM, 0.374 mM and 0.30 mM to be used in the enzyme assay. Inhibitors used in the assay were prepared by dissolving appropriate amount of inhibitor in H₂O to create a 5 mM stock solution which was further diluted to 1 mM and 0.5 mM which were eventually used in the assay.

***In vitro* assay:** Reaction tubes were set up ($V_{\text{final}} = 500 \mu\text{L}$) containing 50 μL 1.0 M acetic acid/sodium acetate buffer, 100 μL of varying concentrations of sub-stock pnpp in the absence of inhibitor (330 μL E-pure H₂O) and 330 μL of two fixed concentrations of inhibitor (1 mM and 0.5 mM). Inhibitor concentrations were determined as described previously.⁴ 20 μL of enzyme (1:1 glycerol/enzyme solution diluted to give $A_{405} = 0.12$) was added to reaction tubes at 30 sec intervals and allowed to react for 15 min. At this time the reaction was quenched by removing 100 μL from the reaction tube and addition to 150 μL 0.5 M KOH in a standard 96-well plate. Absorbance at 405 nm was then recorded and entered into a prepared spreadsheet to determine velocity of the reaction. The one substrate one inhibitor section of Visual Enzymics © of the IgorPro interface was used to determine the inhibition constant (K_i). Substrate and inhibitor concentrations (mM) were entered into the data sheet along with the velocity of the reaction. The standard deviation and mask was set to 1 for all reactions. The data was then fit to competitive, uncompetitive and mixed inhibition models.

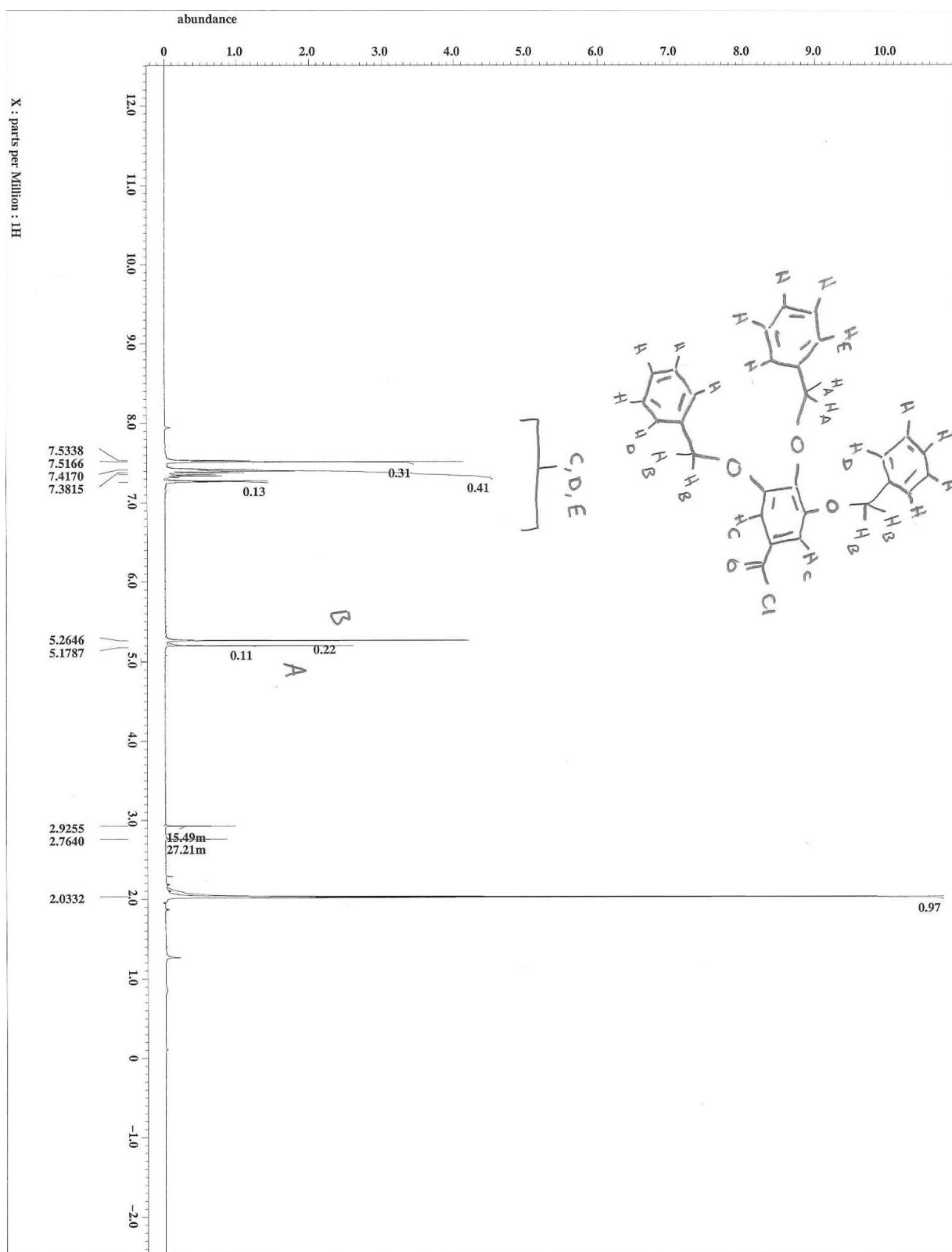
S1. ^1H NMR of Methyl 3,4,5-tribenzyloxybenzoate.



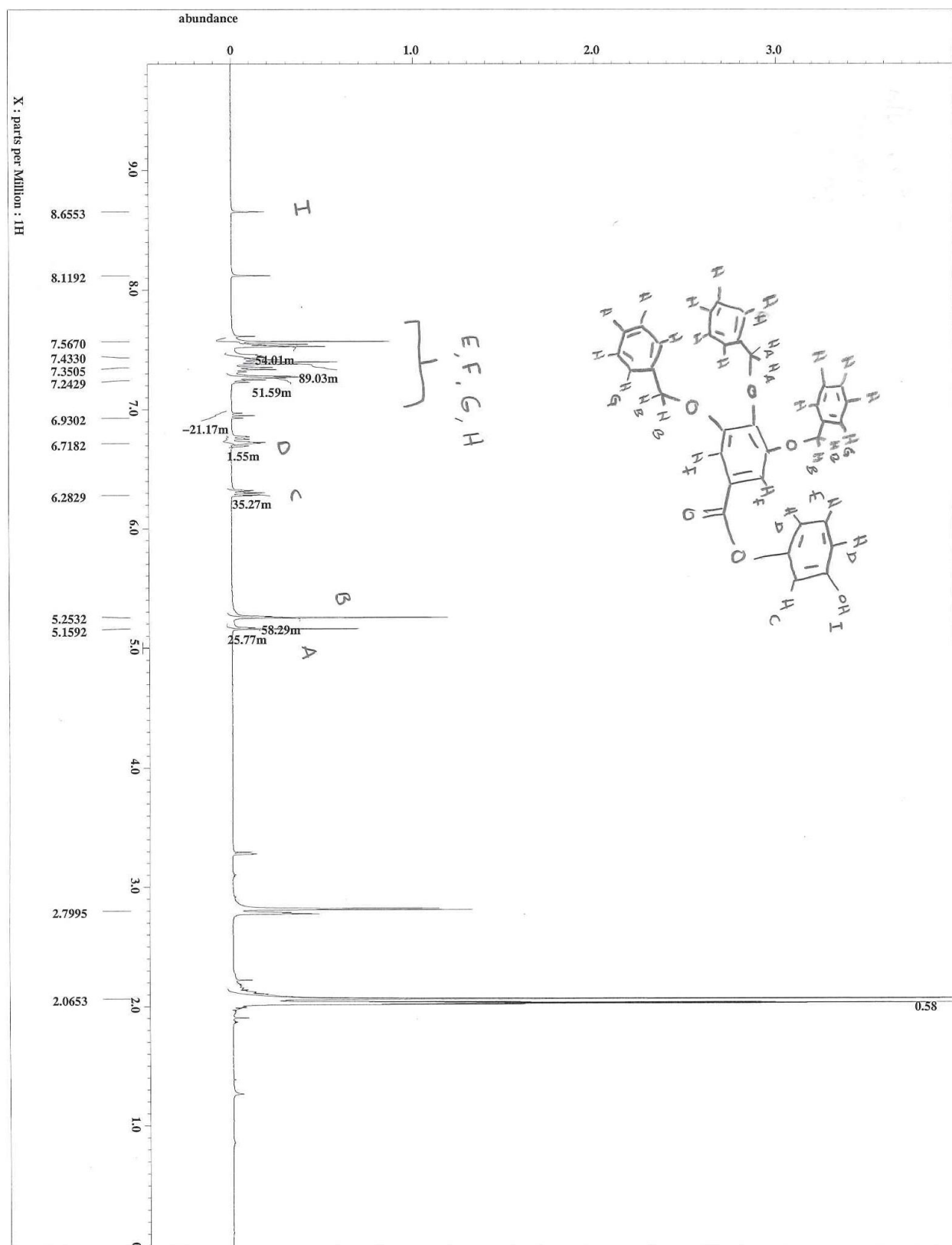
S2. ^1H NMR of 3,4,5-Tribenzyloxybenzoic acid.



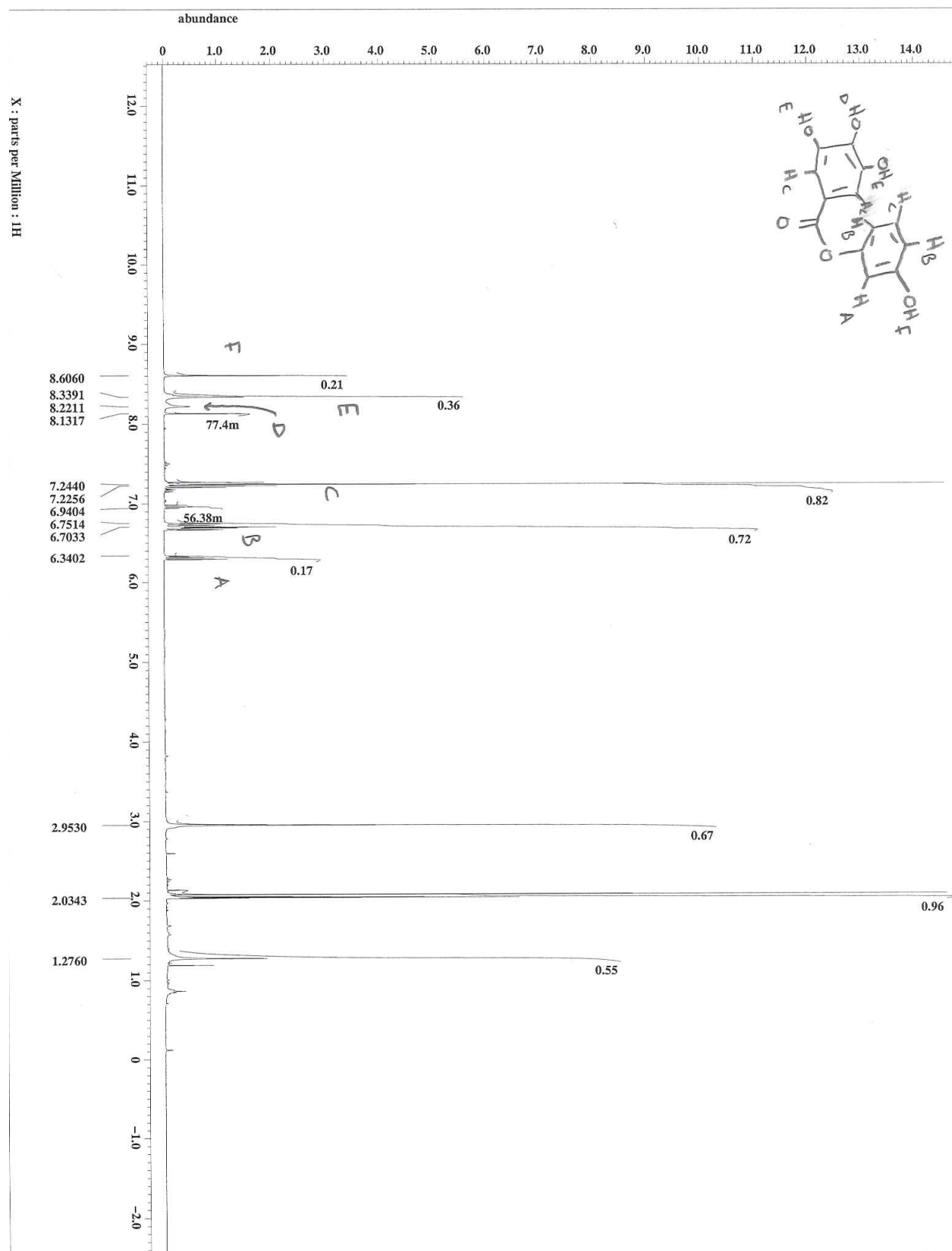
S3. ^1H NMR of 3,4,5-Tribenzyloxybenzoyl chloride.



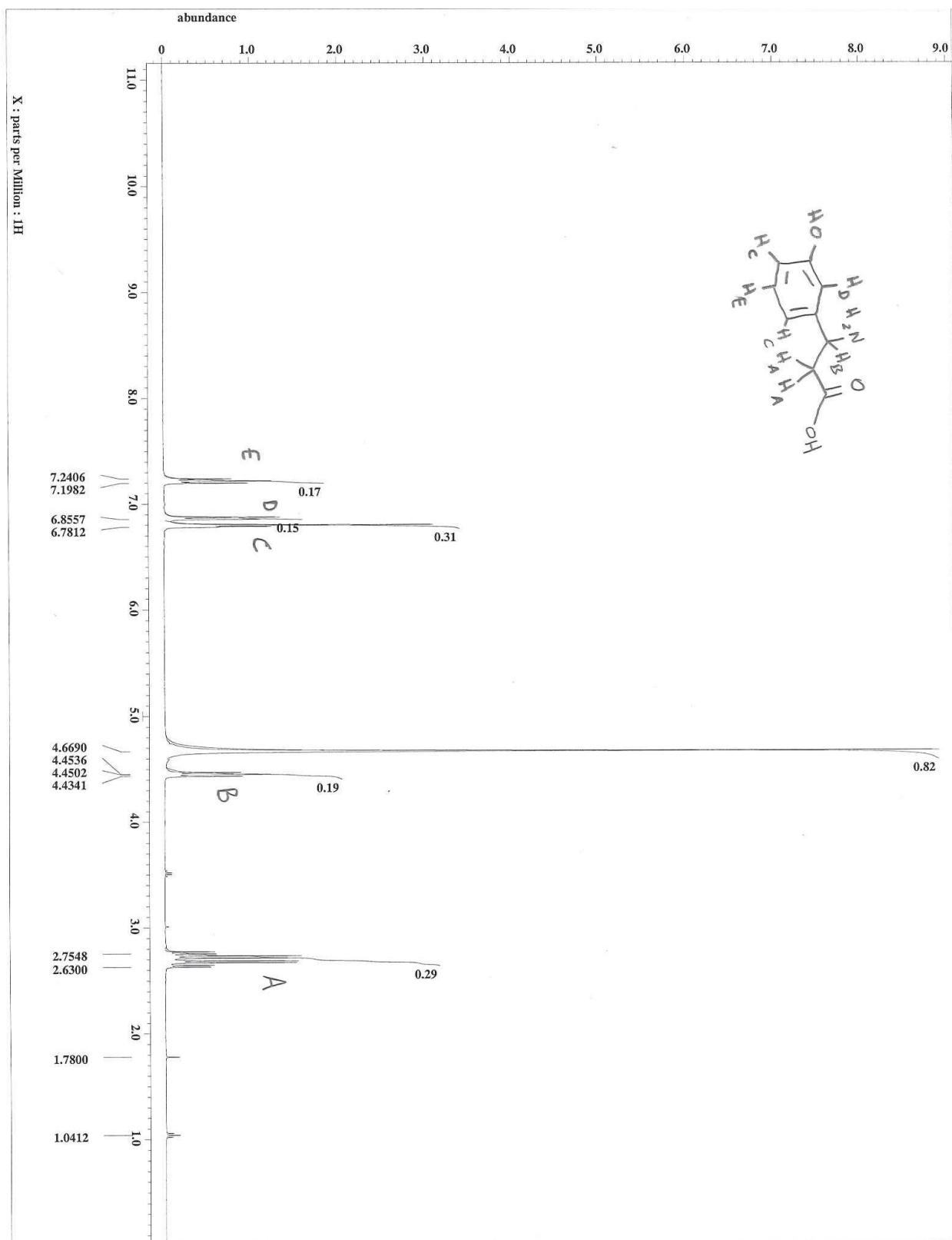
S4. ^1H NMR of 3-Hydroxyphenyl 3,4,5-tribenzyloxybenzoate.



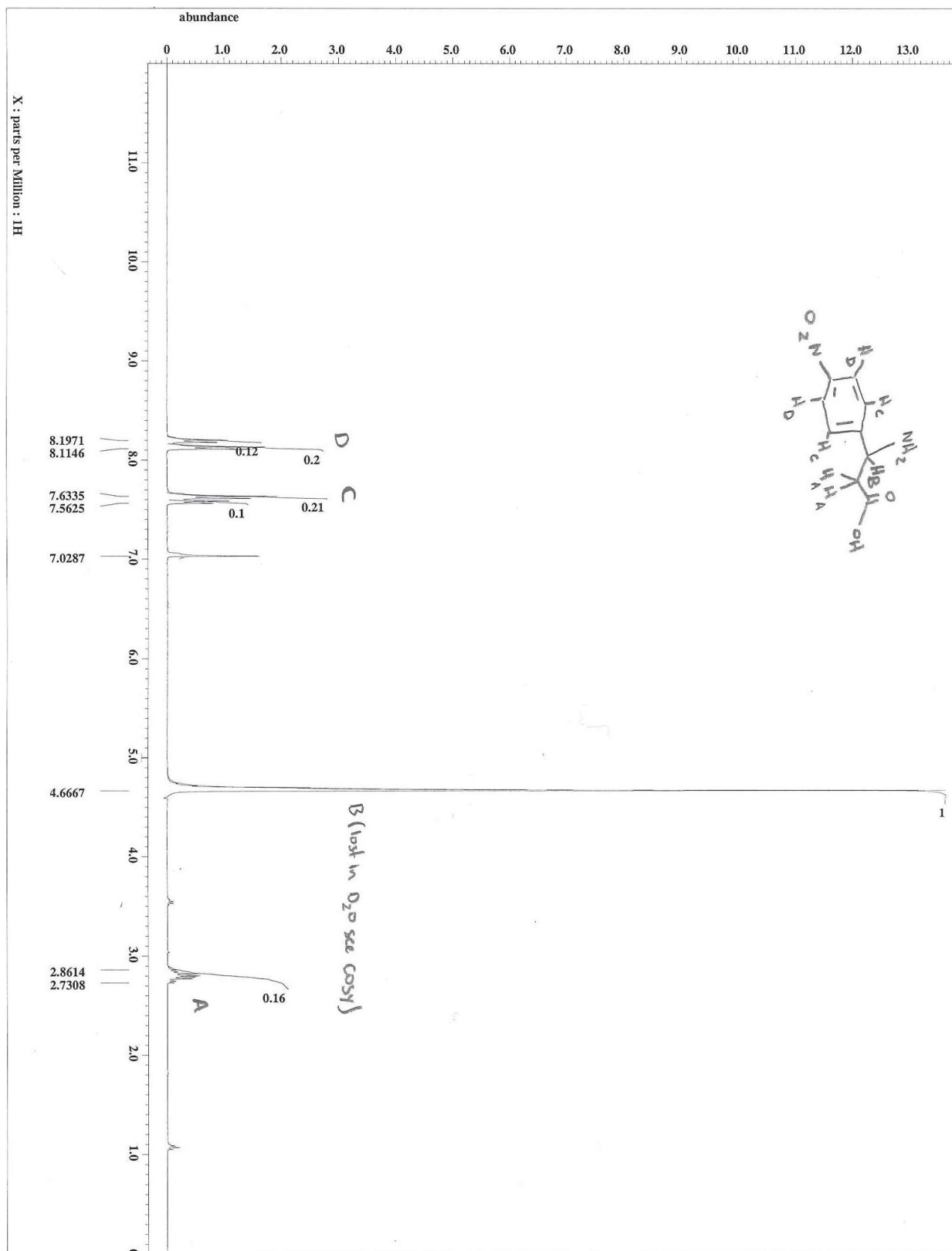
S5. ^1H NMR of 3-Hydroxyphenyl 3,4,5-trihydroxybenzoate.



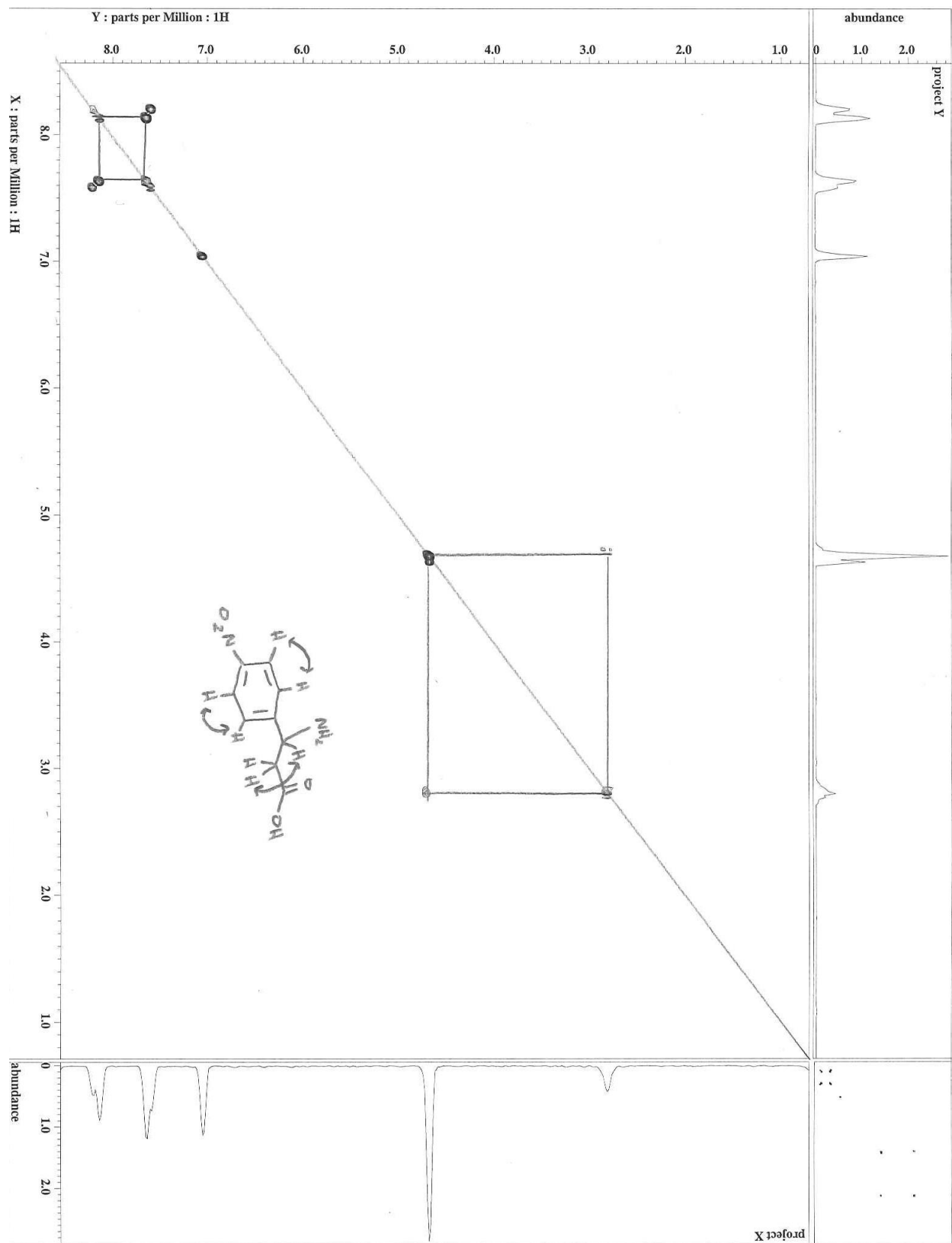
S6. ^1H NMR of 3-amino-3-(3-hydroxyphenyl)propanoic acid.



S7. ^1H NMR of 3-amino-3-(4-nitrophenyl)propanoic acid.



S8. ^1H - ^1H COSY of 3-amino-3-(4-nitrophenyl)propanoic acid.



S9. ^1H MNR of 3-amino-3-(4-methoxyphenyl)propanoic acid.

